Mineralogy and Petrology (1995) 52: 231–255

Mineralogy and Petrology

Geology of the volcanic-hosted Brockman rare-metals deposit, Halls Creek Mobile Zone, northwest Australia. II. Geochemistry and petrogenesis of the Brockman volcanics

W. R. Taylor[1,2], G. Esslemont[3], and S.-S. Sun[4]

[1] Department of Geological Sciences, University College London, London, United Kingdom (present address)
[2] Key Centre for Strategic Mineral Deposits, University of Western Australia, Nedlands, Australia and Geology Department, University of Tasmania, Hobart, Tasmania, Australia
[3] Faculty of Resource Science and Management, University of New England, Northern Rivers Campus, Lismore, N.S.W., Australia (present address)
[4] Australian Geological Survey Organisation, Canberra, Australia

With 5 Figures

Received August 26, 1993;
accepted January 14, 1994

Summary

Lavas and subvolcanic intrusions of the 1.87 Ga Brockman volcanics comprise a cogenetic suite of alkaline, *Qz*-normative, metaluminous trachyandesites, trachytes and trachydacites/rhyolites. They are genetically related to the rare-metal-bearing "Niobium Tuff" which contains extreme enrichments in high-field-strength incompatible elements (av. 1660 ppm Y, 9700 ppm Zr, 3200 ppm Nb, 175 ppm Yb). Neodymium isotopic data indicate the Brockman parent magma was mantle-derived with ε_{Nd}(initial) $\approx +3$, analogous to basaltic magmas generated in some modern intraplate "hot-spot" volcanic provinces. The geochemical evolution and incompatible element enrichments in the Brockman suite can be modelled by AFC processes involving extensive degrees of crystallization and progressive contamination of derivative magmas with granitic/metasedimentary upper crust. The large degrees of crystallization required to derive the more differentiated members of the Brockman suite are best accommodated by a process of "liquid fractionation" resulting in internal compositional stratification of the magma chamber with extreme differentiates such as the Niobium Tuff forming a volatile-enriched "cap" in the magma chamber roof-zone. The high fluorine content of the Brockman magmas played a crucial role in enhancing rare-metal contents by increasing the efficiency of crystal-liquid separation and decreasing mineral-melt K_d's. There appears to be no special role for fluorine-rich fluids in generating the rare-metal enrichments. However, leaching of fluorocarbonate minerals by late hydrothermal solutions,

rather than fractionation of a LREE-selective phase, caused marked LREE-depletion in the Niobium Tuff.

Zusammenfassung

Geologie der an Vulkanite gebundenen Seltene-Metalle-Lagerstätte Brockman, Halls Creek Mobile Zone, Nordwest-Australien. II. Geochemie und Petrogenese der Brockman-Vulkanite

Laven und subvulkanische Intrusionen der 1.87 Mrd. J. alten Brockman-Vulkanite umfassen eine kogenetische Abfolge von alkalinen Qz-normativen Trachyandesiten, Trachyten und Trachydaziten/Rhyoliten. Diese sind genetisch in Beziehung zu dem Seltene-Metalle-führenden "Niob-Tuff", der extreme Anreicherungen an inkompatiblen Elementen hoher Feldstärke führt (im Durchschnitt 1660 ppm Y, 9700 ppm Zr, 3200 ppm Nb, 175 ppm Yb, zu stellen. Nd-Isotopen zeigen, daß das Muttermagma der Brockman-Lagerstätte Mantelursprungs ist mit ε_{Nd} (initial) $\approx +3$, analog zu basaltischen Magmen, die an manchen modernen "intraplate hot-spot" Vulkanprovinzen gebildet werden. Die geochemische Evolution und die Anreicherung inkompatibler Elemente in der Brockman-Abfolge kann durch AFC Prozesse modelliert werden, die extensive Kristallisation und progressive Kontamination der entstehenden Magmen mit granitischer/metasedimentärer Oberkruste beinhalten. Der hohe Grad von Kristallisation der erforderlich ist, um die mehr differenzierten Anteile der Brockman-Abfolge zu erhalten, läßt sich am besten durch einen Prozeß von "liquid fractionation" erklären, der zu einer inneren Stratifikation der Magmenkammer führt, wobei extreme Differentiate, sowie der Niob-Tuff, eine an Volatilen angereicherte Kappe im Dachbereich der Magmenkammer bildeten. Der hohe Fluor-Gehalt der Brockman-Magmen spielte eine wichtige Rolle bei der Anhebung der Seltene-Metalle-Gehalte, und zwar dadurch, daß er die Effizienz der Kristall-Schmelze-Trennung erhöhte und abnehmende Mineral-Schmelze K_d-Werte ermöglichte. Fluor-reiche Fluide scheinen keine spezielle Rolle bei der Bildung der Seltene-Metalle-Anreicherungen zu spielen. Auslaugung von Fluorokarbonaten durch späte hydrothermale Lösungen und nicht die Fraktionierung einer LREE selektiven Phase, bewirkte eine deutliche LREE-Abreicherung im Niob-Tuff.

1. Introduction

Rare-metal mineralization, hosted in a volcaniclastic unit informally termed the "Niobium Tuff", is associated with a suite of well-preserved, trachyte-dominated, alkaline, *Qz*-normative volcanic rocks (lavas, subvolcanic intrusives and volcaniclastics) of the Brockman volcanics. They are located in a ≈ 50 km^2 area of the early Proterozoic Halls Creek Mobile Zone of Western Australia within a zone of low-grade regional metamorphism. Details of the geological and depositional environment, age of emplacement, and petrography of the Brockman volcanics have been discussed by *Taylor* et al. (1995) in the accompanying paper. The mineralogy of the Niobium Tuff has been discussed by *Ramsden* et al. (1993).

A significant feature of the Brockman lavas and the associated Niobium Tuff is their extreme enrichments in incompatible elements, particularly the so-called "rare-metals": Nb, Zr, and Ta (termed the high-field strength elements or HFSE), and the heavy rare-earth elements (HREE) such as Yb. The concentrations of these elements in the most evolved rocks of the suite appear, from a search of the literature, to be the highest known abundances in *Qz*-normative felsic volcanic rocks. In fact, some incompatible elements have abundances more than an order of magnitude greater

than those present in many continental rhyolitic volcanic suites such as the topaz rhyolites of western North America (*Christiansen* et al., 1986), and felsic volcanics of the Kenyan Rift (*Baker*, 1987), which are normally regarded as incompatible-element rich.

The main aims of this investigation are to establish the geochemical affinity of the Brockman volcanics and to determine the nature of the relationship between the least evolved rocks (trachyandesites) and the most evolved, incompatible-element-rich felsic rocks of the Brockman suite. The petrogenetic processes responsible for rare-metal enrichments in the Brockman volcanics and the role of magmatic processes in concentrating the rare-metals in the Niobium Tuff can then be evaluated.

2. Methods

Thirty samples of trachytic volcanic rocks from the Brockman area, including bulk samples of the Niobium Tuff, and a sericitic sedimentary rock underlying the Niobium Tuff were selected for geochemical analysis. Following removal of weathering rinds, and minor vein and vesicle material, samples were ultrasonically cleaned, jaw-crushed to 1–2 mm grain-size, and ~ 100 g splits were ground to a fine powder in an agate ring-mill.

Major and minor elements and some trace elements (Sc, Zn, Ga, Rb, Sr, Y, Zr, Nb, Ba and Pb) were determined by XRF at the University of Western Australia using Norrish-Hutton fusion discs for the major-elements and pressed-powder pellets for the trace elements. Rare-earth elements plus Hf, Ta, Th and U were determined by INAA at Becqueral Laboratories, Sydney. Accuracy of the XRF and INAA methods was established against the incompatible-element-rich NIM-S, NIM-L, and NIM-G South African Bureau of Standards international reference materials. F(luorine) and Be were analysed by NaOH fusion followed by specific-ion electrode determination for F (20 ppm detection limit) and DCP emission spectrographic determination for Be (0.5 ppm detection limit). Sn was analysed by NH_4I fusion/iodine sublimation followed by AAS determination (5 ppm detection limit). Sulphur and CO_2 contents were determined by LECO induction furnace analysis with an accuracy better than $\pm 10\%$ (*R. Chang*, pers. comm.).

Nd isotopic compositions on six samples were determined at the Research School of Earth Sciences, Australian National University, Canberra with a Finnigan MAT 261 mass spectrometer using the experimental procedures described by *Maas* and *McCulloch* (1991). To remove the effects of mass fractionation, reported $^{143}Nd/^{144}Nd$ ratios were normalized to $^{146}Nd/^{144}Nd = 0.7219$. Average $^{143}Nd/^{144}Nd$ ratios for the LaJolla and BCR-1 standards are 0.511872 ± 2 and 0.512653 ± 5 (2σ), respectively. The uncertainty in the measured ε_{Nd} values is ± 0.2 units at the 2σ level.

3. Whole-rock geochemistry

3.1 Major and minor elements

Lavas and subvolcanic rocks

Chemical analyses and CIPW norms of representative samples and averages for the least-altered rocks are presented in Table 1 (a complete listing of analytical data is

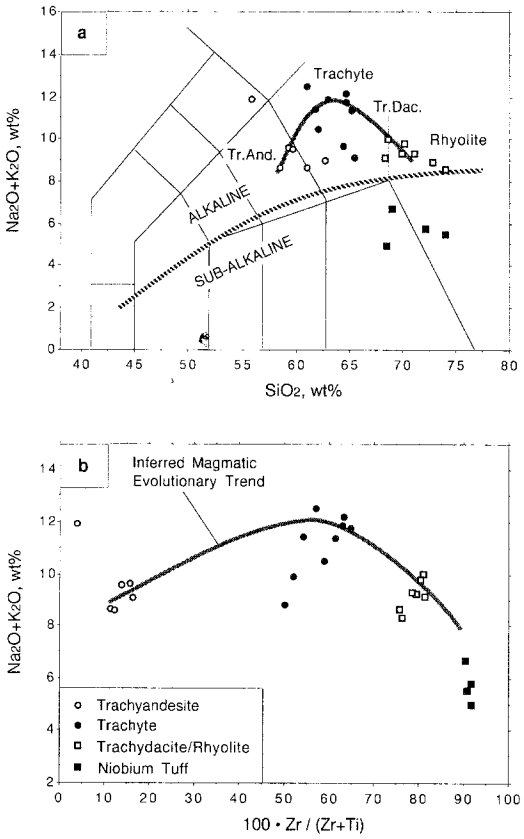

Fig. 1. **a** Total alkalis versus silica (TAS) diagram for the Brockman volcanic rocks normalized on a volatile-free basis. Rock boundaries from *LeMaitre* (1989); *Tr.And.* trachyandesite, *Tr.Dac.* trachydacite. Lower curve is the alkaline/sub-alkaline rock series boundary after *Miyashiro* (1978). The Niobium Tuff composition plots in the sub-alkaline field but has been modified by some alkali loss. Upper curve is an inferred magmatic trend that includes least-altered Brockman lavas. **b** Total alkalis versus zr-number differentiation index showing an inferred magmatic evolutionary trend. Alkali loss is noticeable in some of the trachytes and trachydacites

given by *Esslemont*, 1990). Rock compositions are plotted on a total-alkalis versus silica diagram in Fig. 1a, with various rock classification fields delineated after *LeMaitre* (1989). The Brockman lavas and subvolcanic rocks all classify as alkaline rocks on Fig. 1a using the alkaline/sub-alkaline boundary of *Miyashiro* (1978). Using both chemical and normative criteria, the lavas and subvolcanic rocks can be divided into three broad groups. Following the nomenclature of *LeMaitre* (1989) these are: trachyandesites ($<60\%$ SiO_2), trachytes ($>60\%$ SiO_2, $<10\%$ normative *Qz*) and trachydacites/rhyolites ($>65\%$ SiO_2, $>20\%$ normative *Qz*) which correspond to the petrographic types trachyandesite, trachyte and quartz-trachyte/rhyolite identified by *Taylor* et al. (1995). The trachydacites ($\sim 68\%$ SiO_2), which grade toward rhyolitic compositions with $>70\%$ SiO_2, are more siliceous than indicated from petrographic studies of *Taylor* et al. (1995). For the sake of brevity, these borderline rhyolitic-to-trachydacitic compositions are referred to as trachydacites in the text.

The effects of alteration and metamorphic overprinting are manifest in the Brockman lavas and subvolcanic intrusions mainly in variable total alkali contents (see scatter in Fig. 1a), variable Na_2O/K_2O ratios, and high CO_2 contents (typically 1.0–1.5 wt%). Several rock compositions have $CO_2 > 2$wt% and/or have extreme Na_2O/K_2O ratios; these were rejected from the averages shown in Table 1. One sample (BR15/2, broadly a basaltic trachyandesite composition) has a very high K_2O content (>10 wt%), suggesting metasomatic K_2O introduction; the rock composition has, however, been included in Tables 1 and 2 for comparative pur-

Table 1. *Representative and average major element compositions (with standard deviations) and CIPW norms for Brockman volcanics, the Niobium Tuff, and a sericitic sediment underlying the Niobium Tuff*

Rock:	-BTrA-	--Trachyandesite--			---------Trachyte----------				---Trachydacite/Rhyolite---				----------Niobium Tuff----------				-Sed.-
No.:	BR15/2	BR1/12	Av.(3)	s.d.	BR1/C	BR4/1	Av.(7)	s.d.	BR17/3	BR2/40	Av.(6)	s.d.	BR1/LT	Av.(4)	s.d.	LNbT§	UNbT§	BR1/S
SiO2	53.15	56.31	57.2	(0.9)	60.18	63.38	62.2	(3.5)	67.84	67.19	68.3	(2.8)	68.26	64.8	(6.3)	67.7	65.6	57.56
TiO2	2.15	0.94	0.82	(.10)	0.22	0.21	0.24	(.03)	0.18	0.13	0.16	(.03)	0.17	0.15	(.03)	0.15	0.16	0.47
Al2O3	16.19	15.90	16.0	(0.9)	16.62	15.52	15.7	(1.2)	11.64	12.81	12.4	(0.6)	14.27	13.6	(1.4)	13.3	14.3	23.06
Fe2O3t	5.18	10.26	10.3	(0.6)	4.29	5.48	5.9	(1.0)	6.94	4.43	4.9	(1.1)	1.98	2.6	(0.6)	2.4	2.9	5.18
MnO	0.04	0.14	0.13	(.01)	0.12	0.13	0.12	(.03)	0.21	0.14	0.14	(.04)	0.01	0.06	(.04)	0.05	0.05	0.02
MgO	1.72	1.67	1.4	(0.4)	1.05	0.36	0.8	(0.6)	0.33	0.93	0.5	(0.4)	1.30	1.5	(0.3)	1.2	1.9	1.78
CaO	4.61	2.54	2.4	(0.5)	1.71	1.06	1.2	(0.7)	0.22	0.57	0.6	(0.5)	1.17	3.4	(2.3)	2.7	2.4	0.11
Na2O	0.96	3.72	4.3	(0.8)	4.56	5.38	4.4	(1.2)	2.79	3.81	4.1	(0.7)	0.30	0.7	(0.9)	2.3	0.04	0.25
K2O	10.39	4.63	4.7	(0.7)	6.78	5.68	6.5	(1.9)	6.20	5.55	4.7	(1.2)	4.80	4.6	(1.5)	3.6	5.8	8.17
P2O5	0.74	0.26	0.22	(.04)	0.03	0.02	0.03	(.02)	0.01	0.01	0.01	(.00)	0.01	0.04	(.03)	0.05	0.05	0.10
ZrO2	0.07	0.10	0.11	(.01)	0.30	0.27	0.27	(.04)	0.53	0.43	0.47	(.05)	1.31	1.20	(.11)	1.22	1.31	0.04
Nb2O5	0.01	0.01	0.01	(.00)	0.05	0.05	0.04	(.01)	0.12	0.11	0.12	(.01)	0.45	0.45	(.01)	0.40	0.56	0.03
CO2	1.66	1.79	1.3	(0.5)	1.18	0.25	1.1	(0.6)	0.09	2.18	1.2	(1.1)	1.51	1.3	(0.7)	0.9	0.4	0.54
F	0.05	0.04	0.05	(.03)	0.03	0.04	0.06	(.08)	0.03	0.12	0.32	(.42)	0.77	1.48	(.51)	1.7	2.0	1.53
LOI	4.35	3.83	2.8	(0.8)	3.30	2.29	2.5	(0.6)	1.85	3.40	2.6	(1.1)	3.92	4.8	(2.0)	3.8	3.8	3.80
Total¶	99.61	100.29	100.4		99.20	99.82	99.9		98.85	99.46	100.0		97.63	97.3		98.2	98.0	99.96
CIPW Norm*																		
Qz	0.0	5.9	4.2		1.2	6.0	6.4		24.0	20.0	24.2		46.1	38.6		37.3	40.0	21.2
C	0.0	0.8	0.1		0.0	0.0	0.0		0.1	0.0	0.4		9.0	5.5		5.3	9.1	14.3
Or	64.7	28.3	28.6		41.7	34.3	39.5		37.8	34.1	28.6		30.1	28.0		21.3	34.2	50.1
Ab	6.9	32.5	37.5		40.2	46.5	38.3		24.4	33.5	35.7		2.7	6.1		19.5	0.3	2.2
An	9.6	11.1	10.6		5.1	1.5	4.0		0.8	1.5	0.6		0.1	5.9		0.8	0.0	0.0
Di	7.9	0.0	0.0		2.8	3.1	1.3		0.0	0.4	0.0		0.0	0.0		0.0	0.0	0.0
Hy	0.0	13.3	11.8		5.6	4.7	6.6		8.0	6.8	5.7		5.2	6.1		5.0	7.1	8.6
Mt+Il	6.8	7.1	6.4		2.7	3.2	3.2		3.9	2.6	2.6		1.4	1.5		1.6	1.4	3.4
Ap	1.9	0.6	0.5		0.1	0.1	0.1		<0.1	<0.1	<0.1		<0.1	0.1		0.1	0.1	0.2
Z	<0.1	0.1	0.1		0.4	0.4	0.4		0.8	0.6	0.7		2.0	1.8		1.9	2.0	<0.1
Fl	0.2	0.2	0.2		0.1	0.2	0.3		0.1	0.5	1.4		3.4	6.3		6.9	8.2	0.0
A.I.	0.79	0.70	0.76		0.89	0.97	0.91		0.97	0.96	0.95		0.40	0.45		0.58	0.44	0.40
zr no.	3.6	11.4	13.5		62.9	61.4	58.2		78.4	80.3	78.4		90.5	90.8		90.9	91.0	8.6

§ LNbT = average of 9 whole-rock analyses of the lower Niobium Tuff; UNbT = average of 6 whole-rock analyses of the upper Niobium Tuff; both from core BR-1 (*French* and *Ramsden*, unpubl. data).

¶ Total corrected for oxide equivalent of fluoride.

* Calculated for $Fe_2O_3/FeO = 0.5$; analyses normalized to 100% exclusive of CO_2 and LOI.

Abbreviations: *BTrA* basaltic trachyandesite; *A.I.* agpaitic (peralkalinity) index = molar Na + K/Al; *zr no.* zirconium number (differentiation index) = 100*Zr/(Zr + Ti)

Table 2. *Representative and average trace element compositions (ppm/wt) of Brockman volcanic rocks, the Niobium Tuff, and a sericitic sedimentary rock underlying the Niobium Tuff*

Rock§:	-BTrA-	-Trachyandesite-		--------Trachyte---------			---Trachydacite/Rhyolite---			--Niobium Tuff--		-Sed.-	Enrichment Factors*		
No.:	BR15/2	BR1/12	Av.(3)	BR1/C	BR4/1	Av.(7)	BR17/3	BR2/40	Av.(7)	BR1/LT	Av.(4)	BR1/S	TR/TA	TD/TA	NbT/TA
Be	3.3	4.7	6	5.7	4.7	8	6.6	6.8	12	35	93	23	1.3	2.0	3.8
S	97	<20	47	<20	<20	23	39	20	138	98	369	100	0.5	2.9	7.9
Sc	15	7	5	<1	<1	1	<1	<1	<1	2	<1	11	0.2	<0.2	<0.2
Zn	149	230	203	142	330	303	686	374	615	624	870	178	1.5	3.0	4.3
Ga	28	30	36	44	41	44	50	64	61	114	110	43	1.2	1.7	3.1
Rb	104	65	80	185	195	192	339	349	273	590	484	797	2.4	3.4	6.1
Sr	86	104	112	105	72	66	57	41	54	49	64	55	0.6	0.5	0.6
Y	58	69	73	227	216	197	575	379	472	1661	1210	64	2.7	6.5	16.6
Zr	486	727	766	2239	1999	2005	3926	3183	3475	9666	8873	265	2.6	4.5	11.6
Nb	77	88	92	354	322	284	866	746	821	3125	3176	202	3.1	8.9	34.5
Sn	<5	<5	<5	<5	<5	<5	26	22	24	30	54¶	<5	-	>5.0	>11.0
Ba	5130	2714	2000	564	381	378	542	175	310	1210	823	830	0.2	0.2	0.4
La	86	79	88	329	309	306	412	376	433	19.0	21	58.7	3.5	4.9	0.2
Ce	192	181	199	719	675	651	823	785	836	80.6	109	118.0	3.3	4.2	0.5
Nd	100	94	101	293	278	273	297	270	328	80.2	75	48.4	2.7	3.2	0.7
Sm	19.8	18.5	19.5	54.9	51.7	51	63.0	57.9	65	33.3	38	10.8	2.6	3.3	1.9
Eu	5.7	5.5	5.6	4.0	3.9	3.8	3.6	2.5	3.3	4.3	3.8	1.1	0.7	0.6	0.7
Tb	2.3	2.2	2.4	6.7	6.4	6.1	11.1	9.5	10.5	29.2	27	1.8	2.5	4.4	11.3
Ho	2.5	2.3	2.7	7.9	8.1	7.6	17.0	13.2	15.3	59.0	53	2.1	2.8	5.7	19.6
Yb	4.4	5.7	6.2	18.9	17.3	17.4	41.9	34.6	39.1	175.0	166	4.5	2.8	6.3	26.8
Lu	0.62	0.89	0.94	3.0	2.7	2.5	5.9	5.6	5.9	26.6	24	0.62	2.7	6.3	25.5
Hf	11.6	15.1	16.6	54.9	49.2	49.8	109	103	105	391	378	9.1	3.0	7.0	22.8
Ta	5.8	6.0	5.9	26.0	20.9	20.6	61.9	60.7	61.8	269	253	1.6	3.5	10.5	42.9
Pb	8	18	13	16	18	23	404	68	113	460	208	19	1.8	8.7	16.0
Th	8.3	8.5	9.3	46.4	42.1	40.7	95.7	89.8	106	419	389	24.5	4.4	11.4	41.8
U	<2	<2	<2	2	2	3	13	16	14	57	50	2	>1.5	>7.0	>25.0
(Ce/Yb)N	11.5	8.4	8.4	10.0	10.2	9.8	5.2	5.9	5.7	0.12	0.17	6.9			
Eu/Eu*	0.96	0.97	0.94	0.24	0.25	0.25	0.17	0.13	0.15	0.22	0.18	0.29			

* Enrichment factor = abundance relative to average trachyandesite; *TR* trachyte, *TD* Trachydacite, *NbT* Niobium Tuff.

¶ Average Sn abundance from 6 values reported for the Niobium Tuff by *Yates* and *Pontifex* (1973).

§ BTrA = basaltic trachyandesite

poses. The remaining rocks show quite consistent geochemical characteristics, e.g. similar total alkali, CaO, MgO, and TiO_2 abundances, within the trachyandesite, trachyte or trachydacite geochemical groups (Table 1). Some trachyandesites and trachydacites, however, contain small amounts ($<1\%$) of normative *C* suggestive of minor alkali or Ca^{2+} loss, as may occur during sericitization of alkali feldspar or during albitization of calcic feldspar. This is consistent with their mineralogical composition discussed by *Taylor* et al. (1995).

Notable features of the Brockman lavas and subvolcanic rocks are their quartz-oversaturated and metaluminous to borderline peralkaline character (agpaitic indicies ≈ 0.70–0.97). These characteristics contrast with hawaiite-to-phonolite lineages, encountered in many alkaline shield volcano complexes, which are *Ne*-normative and have lower alumina contents than the Brockman suite. The Brockman suite also differs from strongly peralkaline trachyte-to-comendite/pantellerite lineages, commonly occurring in rift-related shield volcanoes, on the basis lower total alkalis and TiO_2, and higher alumina contents in the Brockman lavas (cf. *Ewart* and *Chappell*, 1989; *Macdonald*, 1987; *Kampunzu* and *Mohr*, 1991). In addition, the Brockman lavas are generally potassic (Na_2O/K_2O weight ratio <1), although the ratios may have been affected to some degree by alteration.

In both the Brockman trachytes and trachydacites, Zr occurs as a minor-element reaching levels in excess of 0.5 wt% ZrO_2. Following *Pearce* and *Norry* (1979), the ratio $100 \cdot Zr/(Zr + Ti)$, or "zr-number", may be used as an index of igneous differentiation in rocks affected by low-grade regional metamorphism. In intraplate magmatic lineages ranging from trachybasalt to trachyte and rhyolite, where zircon fractionation is minimal (e.g. as shown by strong positive correlations on Nb–Zr diagrams), zr-numbers typically vary from ~ 1–3 in the most primitive basaltic magmas of the series to values ~ 60 in the most evolved felsic rocks (e.g. see *Stolz*, 1985). The most primitive rock analysed from the Brockman volcanics, sample BR15/2, has a zr-number of 3.6. The trachyandesites, which have zr-numbers ≈ 10–15, are the next most primitive rock-type. The trachytes, zr-number ≈ 60, and the trachydacites, zr-number ≈ 78, represent highly evolved compositions. With increasing zr-number in the series trachyandesite → trachyte → trachydacite, there are systematic changes in bulk major-element chemistry such as decreasing P_2O_5, Fe_2O_3(tot), MgO, and CaO; increasing SiO_2; and increasing then decreasing total alkalis (see Table 1 and Fig. 1b). These changes suggest the series represents a magmatic lineage related by crystal fractionation and/or other differentiation processes.

Niobium Tuff and underlying sedimentary rocks

As discussed by *Ramsden* et al. (1993), the Niobium Tuff is compositionally variable, reflecting primary compositional differences between the upper pumiceous and lower crystal-bearing zones of the Tuff, sediment admixing in distal portions of the Niobium Tuff, and late-stage devitrification accompanying deuteric alteration. In Table 1, the quoted average Niobium Tuff composition represents the average of both drill-core and surface samples from the upper and lower zones of the Tuff. Whole-rock analyses from *French* and *Ramsden*, unpubl. report (1988), representing the average of several drill-core samples, are also included in Table 1 for comparison.

Although the composition of the Niobium Tuff is somewhat variable (see standard deviations in Table 1), the four average analyses listed in Table 1 show reasonable consistency. As discussed by *Ramsden* et al. (1993), the principal compositional difference between the upper and lower zones of the Niobium Tuff is the higher Na_2O/K_2O ratio of the lower zone which has retained Na_2O in albitized alkali-feldspar microphenocrysts, whereas Na_2O has been removed from the upper zone as a result of sericitization. As a whole, the Niobium Tuff is a *Qz*-normative (*Qz* > 20 wt%), subalkaline (A.I. ~0.4–0.6), and broadly rhyolitic composition on an LOI-free basis. The Niobium Tuff is characterized by a very high zr-number (~91), several weight percent normative *C* due to its high normative fluorite (*Fl*) content, and a high volatile content (≈4 wt% LOI). Although the Niobium Tuff does contain a small proportion of *C* when the norm is calculated on an F-free basis, the original composition cannot be regarded as peraluminous particularly since the Niobium Tuff is partly sericitized (*Ramsden* et al., 1993), and has clearly lost alkalis during devitrification (cf. *Scott*, 1971 and see Fig. 1a). Compared with other fluorine-rich rhyolitic compositions such as topaz rhyolites of North America or ongonites of central Asia (*Christiansen* et al., 1986), the Niobium Tuff is less siliceous, and has higher MgO, CaO and incompatible element contents.

3.2 Trace elements

Levels of incompatible trace element enrichment

The most remarkable feature of the trace element distribution in the Brockman lavas and sub-volcanic rocks is the extreme level of enrichment in HFSE and HREE, and in some other trace elements such as Zn, Sn and Ga. The levels reported in Table 2 for the trachydacites (e.g. Nb ≈ 800 ppm, Y ≈ 500 ppm, Yb ≈ 40 ppm, Th ≈ 100 ppm, Zn ≈ 600 ppm, Sn ≈ 24 ppm, Ga ≈ 60 ppm), are amongst the highest abundances of these elements known from felsic lavas. Covariation between Zr and Nb in various felsic volcanic suites (Fig. 2), show that only the silica undersaturated

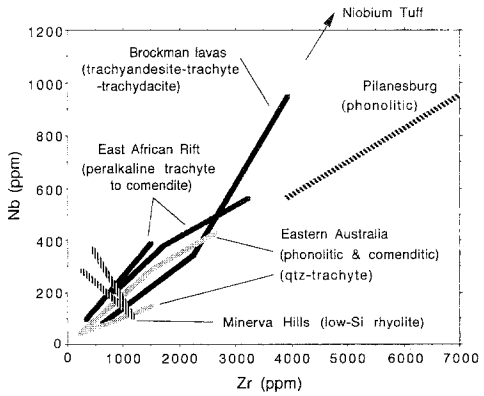

Fig. 2. Trace element plot comparing Zr-Nb evolution of the Brockman lavas with trachytic, comenditic and phonolitic felsic alkaline volanic suites from eastern Australia, southern Africa (Pilanesburg alkaline complex), and the East African Rift (Kenyan segment). Also plotted is the evolutionary trend of the unusual Minerva Hills complex low-silica rhyolites, Queensland, which appear to have fractionated zircon. Data sources: *Ewart* and *Chappell* (1989), *Macdonald* (1987) and *W. Taylor* (unpublished data, Pilanesburg complex)

phonolites of the Pilanesburg complex have comparable Nb enrichments; other *Qz*-normative trachyte suites, such as those from eastern Australian shield volcanoes (*Ewart* and *Chappell*, 1989), are not strongly Nb enriched.

Table 2 lists trace element enrichment factors, relative to the average Table 1 trachyandesite. For the trachydacites, Th, Ta, and U show the greatest enrichments (~10 times) followed by the HREE (~6–7 times). For the Niobium Tuff greatest enrichments are also for Th and Ta (~40 times) and the HREE (~28 times). Some elements such as Pb show variable enrichments in the trachydacites and the Niobium Tuff.

Rare Earth patterns

Chondrite-normalized REE patterns of the Brockman volcanic rock-types and the underlying sericitic sedimentary rock are shown in Fig. 3. Of the lavas, the least evolved trachyandesites show slight LREE enrichment over HREE with $(Ce/Yb)_N \approx 8.5$, and lack an Eu-anomaly. The trachytes, with $(Ce/Yb)_N \approx 10$, have a slightly steeper pattern and show a significant Eu-anomaly ($Eu/Eu^* \approx 0.25$). The trachydacites show greater REE enrichments coupled with more negative Eu anomalies ($Eu/Eu^* \approx 0.15$), and have a flatter REE pattern, $(Ce/Yb)_N \approx 5–6$, compared to the trachytes. Relatively flat REE patterns are a common feature of evolved, low Eu/Eu* rhyolites and some F-rich, topaz-bearing rhyolites and granitoids (e.g. *Ewart* et al., 1985; *Hildreth*, 1979; *Christiansen* et al., 1984, 1986; *Nabelek* and *Russ-Nabelek*, 1990), but they are not typical of peralkaline rhyolites (*Christiansen* et al., 1986). According to *Baker* and *McBirney* (1985), flat REE patterns may arise in these rocks from fractionation of LREE-rich accessory phases such as allanite.

The REE pattern of the Niobium Tuff is unusual in that it shows extreme HREE enrichment (≈800 times chondritic abundance) and marked LREE depletion relative to the HREE. Additionally, a small positive Ce-anomaly is evident in some samples. These features are present in drill-core and surface samples of both the upper and lower zones of the Niobium Tuff and are therefore not related to recent surficial weathering. LREE depletion in the Niobium Tuff could conceivably arise from some primary (e.g. magmatic) process or a secondary process perhaps related to ore mineral formation. If the LREE depletion was caused by secondary processes

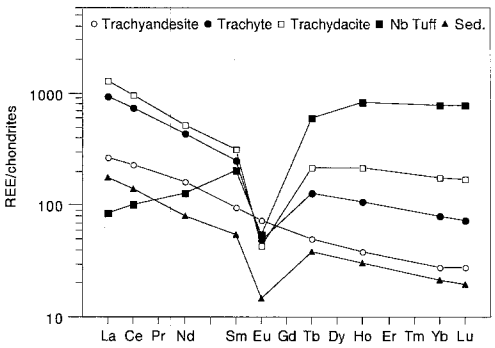

Fig. 3. Chondrite-normalized REE plot for average Brockman volcanic rocks, and a sericitic sedimentary rock immediately underlying the Niobium Tuff. Note the proportionately greater HREE enrichment relative to the LREE for the more differentiated trachydacite lavas and the extreme LREE depletion and HREE enrichment of the Niobium Tuff

Table 3. *Nd Isotope results*

Sample No.	Rock-type	$^{143}Nd/^{144}Nd$ (±2σ)	Sm (ppm)	Nd (ppm)	$^{47}Sm/^{144}Nd$	ε_{Nd} meas.	ε_{Nd} initial
BR1/12	Trachyandesite	0.511781±6	18.02	94.54	0.11524	-16.96	+2.6
8759-8021†	Trachyte	0.511675±6	40.89	227.7	0.10857	-19.01	+2.1
BR17/3	Trachydacite	0.511940±6	50.77	233.7	0.13134	-13.84	+1.8
8759-8001*	Niobium Tuff	0.514966±6	38.36	60.61	0.38296	+45.21	+0.4
8759-8001	Duplicate	0.514896±6	37.08	59.68	0.37583	+43.81	+0.7
BR1/LT	Niobium Tuff	0.515911±8	55.46	73.17	0.45863	+63.61	+0.7
BR1/LT	Duplicate	0.515938±7	55.62	73.31	0.45910	+64.14	+1.2
BR1/S	Sediment	0.511509±6	10.56	52.13	0.12247	-22.25	-4.5

† Brockman trachyte (zr no. = 56.3), sampled by *Buckovic* (1984).
* Niobium Tuff sample dated by *Taylor* et al. (1995)

then the sericitic sediment immediately underlying the Niobium Tuff cannot have been affected since its REE pattern shows no apparent LREE depletion (Fig. 3). A possible primary origin for the LREE-depletion in the Niobium Tuff via accessory phase fractionation is considered below.

Nd isotopic ratios

Initial Nd isotopic ratios (i.e. ε(Nd) corrected to 1870 Ma) for selected Brockman volcanic rocks, including two samples of the Niobium Tuff are given in Table 3. With increasing degree of evolution from trachyandesite to Niobium Tuff, ε_{Nd}(initial) values decrease in regular fashion from $+2.6$ to $\approx +0.7$, respectively. The large present-day ε_{Nd} value of the Niobium Tuff ($+44$ to $+64$) is consistent with long-lived Nd depletion relative to Sm indicating that LREE-depletion in the Niobium Tuff was not a relatively recent (e.g. Tertiary) event. The positive ε_{Nd}(initial) signature of the Brockman volcanics as a whole, indicates that they do not represent partial melts of relatively LREE-enriched Archean or early Proterozoic crustal materials, and that their parent magma is likely to be of mantle derivation. Nevertheless, the ε_{Nd}(initial) variation with increasing degree of evolution suggests either (a) that the Brockman magmas were progressively contaminated with crustal materials of lower ε_{Nd} during their evolution, indicating a role for crustal assimilation processes in their genesis, or (b) that an incorrect age was used to determine the initial ratios. The former case is supported by the presence of granitic and metasedimentary xenoliths and older, crustally-derived zircon xenocrysts within the Niobium Tuff and other Brockman volcaniclastic units (*Taylor* et al., 1995). In the case of hypothesis (b), it can be shown that the Nd isotopic data for the Niobium Tuff, trachyandesite BR1/12, and trachyte 8759-8021 yield a common ε_{Nd}(initial) value $\approx \pm 1.7$ for a 1815 Ma age. This date is some 55 Ma younger than the 1870 ± 4 Ma U/Pb zircon age determined on the Niobium Tuff (*Taylor* et al., 1995) and as such is well outside any uncertainty that can be attributed to the SHRIMP zircon dating; hypothesis (b) can therefore be reasonably rejected.

The single Nd isotopic measurement undertaken on the sericitic sedimentary rock immediately underlying the Niobium Tuff gives initial $\varepsilon_{Nd} = -4.5$, typical of

early Proterozoic sedimentary rocks from northern Australia (*S.-S. Sun*, unpubl. data).

4. Petrogenetic modelling

4.1 Trace element evidence for cystal-liquid fractionation

Studies of chemically zoned eruptive units provide abundant evidence that crystal-liquid fractionation is the principal mechanism of igneous differentiation leading to formation of felsic rocks from intermediate to basic parental magmas (e.g. *Wörner* and *Schminke*, 1984; *Baker* and *McBirney*, 1985). In some cases, anomalous trace element variations have led to the suggestion that additional, non-crystal-liquid processes, e.g. thermogravitational diffusion assisted by volatile complexation, volatile transfer, and liquid immiscibility, may be involved (*Hildreth*, 1979; *Mahood*, 1981). But in many cases these anomalies can be satisfactorially explained by fractionation of accessory phases such as allanite, zircon, apatite, etc. (*Cameron*, 1984; *Baker* and *McBirney*, 1985). For the Brockman volcanics, which show extreme enrichments in incompatible elements, implying extensive and possibly unrealistic degrees of fractional crystallization, it is conceivable some of these non-crystal-liquid processes could be responsible for the observed enrichments. It is therefore important to determine whether element variation in the Brockman volcanic suite is compatible with the operation of crystal-liquid fractionation processes alone.

An important criterion for establishing whether members of a comagmatic suite are genetically related is that they should exhibit strong inter-element correlations on chemical variation diagrams. If the common genetic process was dominantly fractional crystallization, then binary logarithmic plots of incompatible trace elements are the most useful for demonstrating this relationship even where moderate degrees of crustal assimilation are involved (i.e. in assimilation-fractional crystallization or AFC processes). This derives from the standard Rayleigh crystal fractionation equation expressed in terms of the relative concentration of two elements (*Christiansen* et al., 1984). If one of these elements, e.g. element "i", is a highly incompatible element, i.e. has a bulk distribution coefficient (D_i) that approaches zero, then the equation takes the form:

$$\log[C_{L(j)}] = (1 - D_j) \cdot \log[C_{L(i)}] + (\text{constant})$$

where $C_{L(j)}$ = concentration of trace element j in the residual liquid, and D_j = bulk distribution coefficient for element j. Thus an igneous suite derived by closed-system crystal fractionation processes will show a high degree of correlation between element j and highly incompatible element i on a log-log plot. The only qualification is that D_j should remain constant during a fractionation stage since the slope of the line is equal to $(1 - D_j)$. If several fractionation stages are involved, and D_j varies during those stages, then the inter-element correlations will consist of a series of linear segments of different slopes. If the igneous suite is derived by AFC processes, it can be demonstrated from the equations presented by *DePaolo* (1981), that a similar linear relationship holds for an incompatible element "j" over a large fractionation range provided the ratio of assimilation rate to fractionational crystallization rate ("r-factor") is less than about 1, and the concentration of element j in the assimilant does not exceed that in the parent magma.

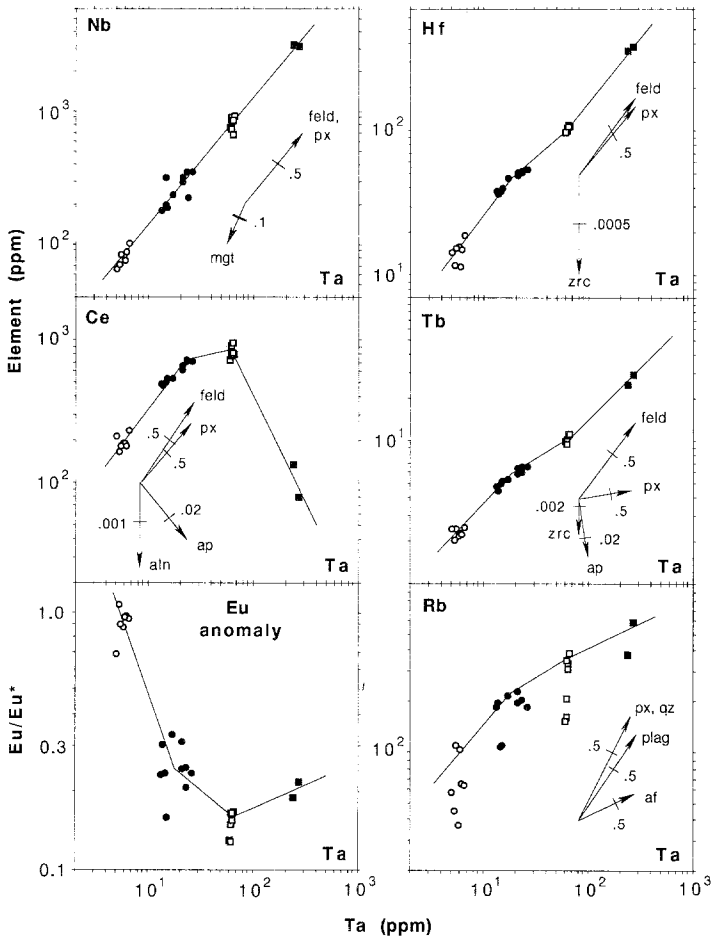

Fig. 4. Binary logarithmic plots relative to Ta showing trace element abundances of selected HFSE and REE elements plus the feldspar compatible elements Eu (expressed as the Eu-anomaly or Eu/Eu*) and Rb. Symbols for the different rock types are the same as Fig. 1. Fractionation vectors, calculated using the crystal-liquid K_d's in Table 5, are indicated for various minerals following *Pearce* and *Norry* (1979). Mineral symbols are as follows: *feld* feldspar; *plag* calcic feldspar; *af* alkali feldspar; *px* pyroxene; *mgt* titanomagnetite; *ap* apatite; *qz* quartz; *zrc* zircon; *aln* allanite. The magnitude of the vectors correspond to 70% crystallization (1-F = 0.7) for *feld*, *px*, *plag*, *af* and *qz*; 20% crystallization (1-F = 0.2) for *mgt*; 3% crystallization (1-F = 0.03) for *ap*; 0.2% crystallization (1-F = 0.002) for *aln*; 0.1% crystallization (1-F = 0.001) for *zrc* (Hf vs Ta) and 1% crystallization (1-F = 0.01) for *zrc* (Tb vs Ta). Tick marks give selected degrees of crystallization (expressed as 1-F values) along the vectors. The diagram shows that the Brockman volcanics comprise a cogenetic suite that can be related by crystal fractionation. Three differentiation stages can be recognized from the slopes of the best fit lines: trachyandesite → trachyte; trachyte → trachydacite, and trachydacite → Niobium Tuff

In Fig. 4, Ta is used as element "i" due to its highly incompatible behaviour in felsic alkaline systems (*Stolz*, 1985; *Mahood* and *Stimac*, 1990). The REE and HFSE are useful as element j (Nb, Hf, Ce, Tb and Eu variation shown in Fig. 4) since they tend to retain primary magmatic abundances even in strongly altered volcanics, and in the case of the Brockman volcanics, have high abundances with respect to any

possible granitic or metasedimentary contaminants. Figure 4 shows that for Nb a strong inter-element correlation exists ($r^2 \approx 0.99$) that spans the full compositional range between the trachyandesites and the Niobium Tuff. Such a strong linear relationship is expected if Nb and Ta abundances are related by crystal-liquid processes in which D_{Nb} remains essentially constant during fractionation. Additionally, the steep slope and mineral vector orientations on the Nb–Ta diagram show that Nb–Ta inter-element variation is not strongly influenced by any major fractionating phases.

Plots of the HREE (e.g. Tb) and other HFSE elements (e.g. Hf) also show strong positive correlations versus log(Ta) ($r^2 \approx 0.98$) but three linear segments of slightly differing slope are discernible in these plots. These segments suggest there were three different stages of magmatic evolution (i.e., trachyandesite → trachyte, trachyte → trachydacite, trachydacite → Niobium Tuff) in which bulk distribution coefficients changed (e.g. due to variations in the proportions or nature of fractionating phases) and/or changes in the rate of assimilation of crustal components. For Ce, three segments are also observed but there are significant changes of slope that suggests Ce behaved compatibly during the latter stages of fractionation.

Figure 4 also shows variations for the more mobile feldspar compatible elements Rb and Eu (plotted as Eu/Eu* ratio). Although exhibiting some scatter, it is clear that Rb behaves incompatibly but is less enriched in the more evolved liquids suggesting involvement of alkali feldspar as a later fractionating phase. On the other hand, Eu/Eu* variation versus log(Ta) indicates strongly compatible behaviour for Eu during the trachyandesite → trachyte and trachyte → trachydacite stages consistent with dominant control by calcic feldspar (plagioclase or anorthoclase) fractionation.

An important feature of both Figs. 1b and 4 is the clustering of data points into discrete fields based on rock-type, i.e. there are compositional gaps in the differentiation sequence. Such behaviour could reflect primary magma zonation in a subvolcanic magma chamber (see below) or could reflect bias in the sampling of magmas to the surface, e.g. as may arise from density contrast between differently evolved liquids. It is also clear from geological mapping of the Brockman volcanics (*Taylor* et al., 1995), that there are differences in the timing and environment of eruption of the different rock-types (e.g. the least evolved trachyandesites were erupted somewhat later than the trachytes and trachydacites), indicating the Brockman suite probably did not originate in a single eruptive event from a compositionally-zoned magma chamber. Nevertheless, it has been established from studies of igneous differentiation that there is usually little difference in the chemical evolutionary trends within a single zoned magma body and those of cogenetic suites erupted over relatively long time periods in the form of separate eruptive units (*Baker* and *McBirney*, 1985). In the case of the Brockman volcanics, the data presented in Fig. 4 clearly establishes a genetic connection amongst all the rock-types including the Niobium Tuff composition.

4.2 Major element modelling by FC and AFC processes

Mass-balance calculations can be undertaken to determine the feasibility of deriving the Brockman volcanic rocks by fractional crystallization (FC) and AFC processes from a least evolved trachyandesitic liquid. In fresh volcanic rocks, such calculations

can generally provide a rigorous test of fractional crystallization models. In the Brockman volcanics, however, phenocryst compositions cannot be determined due to poor preservation of primary igneous minerals; and alkali-loss, albitization and carbonation have affected rock compositions. Although the Niobium Tuff is more extensively altered than any of the lavas, *Christiansen* et al. (1986) showed that secondary processes, including devitrification, do not normally affect concentrations of the petrogenetically important elements in rhyolitic tuffs. Exceptions are elements such as F and alkalis that are readily mobilized in the post-eruption environment. Despite these problems, it is possible to model major and minor element evolution even in partially altered rocks to provide solutions that are consistent with petrographic observations, immobile trace element distributions and isotopic data. The geochemical modelling of AFC processes, however, may not necessarily yield a unique solution due to the large number of variables involved.

Major- and minor-element FC and AFC modelling was undertaken for the three evolutionary stages (i.e. trachyandesite → trachyte, trachyte → trachydacite, and trachydacite → Niobium Tuff) using a least-squares computer program incorporating the AFC equations of *DePaolo* (1982). Average major-element whole-rock compositions (Table 1), normalized to 100% on a CO_2, H_2O, and F absent basis, were used as the parent and daughter compositions in the calculations. The LNbT average analysis (Table 1) was used in the calculations as the target daughter composition for the trachydacite → Niobium Tuff stage since this composition probably best reflects original alkali contents. Because of phenocryst alteration in the Brockman volcanics (*Taylor* et al., 1995), the compositions of feldspars and pyroxenes were entered in the calculations as solid-solution endmembers but mixing of these components was constrained within solid-solution limits of these phases from natural trachytes and rhyolites. Quartz, titanomagnetite and apatite were included as additional phases to account for SiO_2, TiO_2 and P_2O_5 variation.

For the AFC calculations, a crustal assimilant composition consisting of 80% 'granite' and 20% 'shale' (see Table 4) with an ε_{Nd} value of -5 was used in the first series of calculations (AFC-1). The assimilant represents an approximation of the chemical and isotopic composition of the assumed late Archean to earliest Proterozoic upper crustal basement in which the Brockman magma chamber resided (*Taylor* et al., 1995), with chemical compositions taken from the average values reported by *Taylor* and *McClennan* (1985). The 80 : 20 ratio of granite to metasediment is based on the proportions of crustal xenoliths encountered within the Brockman volcanics and this is supported by the high abundance of igneous-type zircons with ~2.5 Ga SHRIMP U–Pb ages relative to zircons of older sedimentary origin (~1.9 Ga age) which occur as xenocrysts within the Niobium Tuff.

Using the proportions of fractionating phases calculated with the FC model as an initial estimate, the r-factor was varied to achieve the desired ε_{Nd} value of the daughter liquid then the F values and proportions of phases were 'fine-tuned' to achieve a minimum residual for the major elements. Zircon and allanite were incorporated into the AFC calculations as HFSE and LREE-selective accessory phases, respectively, to improve agreement between calculated and actual trace element distributions (see below). Both these phases are present as minor or trace minerals within the trachytes (*Ramsden* et al., 1993).

For the trachyandesite → trachyte stage it became clear that a good fit could not be achieved for the proposed assimilant. Because the trachyandesite represents the

longest-lived liquid in the magma chamber it was considered that its composition could be modified by mixing with more-evolved liquids already present in the chamber. Accordingly, a second assimilant composition representing a mixture of crust and a hypothetical evolved magma contaminant (modelled on 40% granite, 10% shale and 50% trachydacite with $\varepsilon_{Nd} = -1.6$) was included in the calculations (AFC-2). Although not well constrained from natural observation, this composition has been used here to provide some indication of the likely effects of mixing more-evolved and less-evolved liquids.

Results of the major element modelling for the three fractionation stages (Table 4) show that the AFC models in general yield an acceptible fit (i.e. sum of squares of residuals $\sum r^2 < 1$). It should be noted, however, that in this case the fit will be better than in many 'fresh' volcanic suites because phenocryst compositions are not tightly constrained. The FC and AFC modelling yields results that are not greatly different either in terms of the amount of crystallization required or the proportions of fractionating phases. The trachytes can be generated by $\approx 70\%$ crystallization of the trachyandesite melt involving fractionation of calcic feldspar and ferrohypers-

Table 4. *Results of least-squares FC and AFC modelling*

Trachyandesite to Trachyte					Trachyte to Trachydacite			Trachydacite to Niobium Tuff			Assimilant Compositions		
	Target	FC	AFC-1	AFC-2	Target	FC	AFC-1	Target	FC	AFC-1		1*	2†
SiO2	64.4	64.2	64.8	64.6	71.4	71.3	71.5	71.0	70.9	71.1	SiO2	71.8	71.6
TiO2	0.25	0.24	0.25	0.26	0.17	0.18	0.17	0.16	0.16	0.17	TiO2	0.27	0.22
Al2O3	16.3	16.2	16.3	16.2	13.0	12.9	13.4	13.9	12.9	13.9	Al2O3	15.2	14.1
FeOt	5.5	5.3	5.6	5.4	4.6	4.7	4.3	2.3	2.2	2.3	FeOt	2.1	3.4
MgO	0.8	0.9	1.0	0.7	0.5	0.4	0.6	1.3	1.1	1.3	MgO	0.9	0.7
CaO	1.2	1.3	1.6	1.3	0.6	0.4	0.6	2.8	2.6	2.2	CaO	1.5	1.0
Na2O	4.6	4.6	4.3	4.5	4.3	4.5	4.1	2.4	2.9	2.8	Na2O	3.3	3.8
K2O	6.7	6.8	5.9	6.7	4.9	4.8	4.8	4.8	5.3	5.0	K2O	4.9	4.9
P2O5	0.03	0.04	0.04	0.06	0.01	0.01	0.01	0.05	0.04	0.07	P2O5	0.08	0.05
ZrO2	0.27	0.44	0.20	0.32	0.47	0.86	0.55	1.3	1.9	1.1	ZrO2	0.03	0.25
E(Nd)	2.1	2.6	2.1	2.1	1.8	2.1	1.8	0.7	1.8	0.7	E(Nd)	-5.0	-1.6
Liq. remaining (F) and assimilation rate (r):													
F		0.25	0.42	0.32		0.32	0.31		0.24	0.19	Trace elements (ppm):		
r		0.00	0.24	0.08		0.00	0.23		0.00	0.31			
Weight proportions of fractionating phases:											Sn	5	14
quartz		-	-	-		-	-		0.2499	0.2487	Sr	150	102
Ca.feld		0.7487	0.7283	0.7333		0.3433	0.3500		-	-	Ba	800	555
alk.feld		-	-	-		0.5500	0.5452		0.6841	0.6893	Eu	0.65	2
Ti-mgt		0.0415	0.0430	0.0390		0.0500	0.0470		0.0520	0.0499	Ga	22	42
opx		0.1774	0.1923	0.1928		0.0354	0.0349		0.0140	0.0090	Be	4	8
cpx		0.0256	0.0277	0.0278		0.0204	0.0201		-	-	Rb	150	212
ap		0.0068	0.0087	0.0070		0.0009	0.0012		-	-	La	29	231
zircon		-	-	0.0001		-	0.0004		-	0.0001	Ce	60	448
allanite		-	-	-		-	0.0012		-	0.0030	Nd	31	180
Sum Sqs Residuals:		0.0848	1.1012	0.1239		0.3192	0.4487		1.9992	0.7336	Sm	7	36
Phase Compositions:											Tb	1.15	5.83
Feld:	Ab54An14Or32				Ab59An15Or26,		Ab36Or64	Ab60Or40			Y	40	256
Px:	En27Fs73,		En14Fs36Wo50		En62Fs38,		En31Fs19Wo50	En69Fs31			Yb	3.6	21.4
Ti-mgt:	Ulv80Mgt20				Ulv18Mgt78			Ulv11Mgt89			Lu	0.54	3.22
Selected trace elements (ppm):											Hf	9.5	57.3
Rb	192	233	204	224	273	286	311	484	471	443	Nb	42	431
Nd	273	253	161	231	328	796	342	75	1341	69	Ta	2.8	32.3
Yb	17.4	18.4	12.5	17.3	39.1	51.2	41.4	166	159	177	Th	16	61
Hf	50.0	63.4	42.0	50.4	105	155	63	378	427	376	U	3.5	8.8
Nb	284	312	207	327	821	762	779	3176	2773	3146			
Ta	20.6	20.7	13.7	22.4	61.8	57.2	58.8	253	218	253			
Th	40.7	36.6	28.6	39.6	106	129	103.0	389	441	174			

* Assimilant-1 = 80% granite + 20% shale

† Assimilant-2 = 40% granite + 10% shale + 50% trachydacite

Average granite and shale compositions after *Taylor* and *McClennan* (1985)

thene with minor titanomagnetite, clinopyroxene and apatite. The trachydacite can be derived by ≈70% crystallization of the trachyte involving fractionation of largely calcic feldspar and alkali feldspar with minor titanomagnetite, hypersthene, clinopyroxene and zircon. Finally, the Niobium Tuff can be generated as the residual liquid from ≈75–80% crystallization of the trachydacite in which quartz and alkali feldspar are the major fractionating phases and hypersthene, titanomagnetite and allanite are minor phases. The AFC modelling shows that progressively greater degrees of assimilation are required at each evolutionary stage with r-factors varying from 0.08 to 0.31 (Table 4).

4.3 Trace element modelling by AFC processes

The major-element FC and AFC models may be quantitatively tested against trace element abundances to test the suitability of these models provided accurate crystal-liquid partition coefficients (K_d's) exist for the system under investigation. *Green* et al. (1992) have shown recently that crystal-melt partition coefficients for the LILE and HFSE are markedly lower in F-bearing silicic systems compared with F-absent systems. It is therefore important in modelling the Brockman volcanics that K_d's are obtained from halogen-rich compositions. Fortunately, K_d data for most phases of interest have recently become available for F and Cl-bearing trachytes and related silicic alkaline rocks (*Francalanci*, 1989; *Mahood* and *Stimac*, 1990; *Congdon* and *Nash*, 1991). Partition coefficients for hypersthene are not available from the above sources, and they were estimated from K_d data for clinopyroxene within constraints provided by rhyolite-hypersthene pairs from the Bishop Tuff (*Hildreth*, 1979). Pre-

Table 5. *Crystal-Melt Partition Coefficients (K_d's) used in this study**

	Qtz	Ca-Fsp	Alk-Fsp	Hyp¶	Ti-Mgt	Ap	Zircon	Allanite
Ba	–	2.8	1.0	0.02	0.03	0.45	–	20
Sr	–	2.5	0.8	0.1	0.15	5	–	100
Eu	–	1.2	0.6	0.8	0.07	30	–	81
Ga§	–	1.0	0.6	0.1	0.10	0.1	–	–
Be§	0.1	0.9	0.3	0.1	0.01	0.2	–	–
Rb	–	0.3	0.9	0.006	0.04	0.2	–	–
La	–	0.07	0.0007	0.14	0.07	27	1	820
Ce	–	0.035	0.0005	0.24	0.07	31	1	635
Nd	–	0.018	0.0004	0.44	0.07	34	1	467
Sm	–	0.009	0.0004	0.8	0.08	38	5	205
Tb	–	0.0035	0.0002	0.95	0.07	30	50	71
Ho	–	0.003	0.0002	0.83	0.07	20	200	25
Y	–	0.003	0.0002	0.76	0.08	17	250	15
Yb	–	0.003	–	0.7	0.05	10	400	9
Lu	–	0.0024	–	0.7	0.08	7	450	8
Hf	–	0.001	–	0.1	0.3	0.07	1600	–
Nb	–	0.001	–	0.02	2.8	0.05	5	–
Ta	–	0.001	–	0.02	2.2	0.05	5	–
Th	–	0.001	–	0.005	0.02	1.6	60	168

* Listed in order of compatibility with calcic feldspar.
Data sources: *Mahood* and *Stimac* (1990), *Francalanci* (1989), *Brooks* et al. (1981), *Hildreth* (1979), *Sawka* and *Chappell* (1988).

— K_d of 0.0001 assumed.

¶ K_d's for hyperthene estimated at half the value for clinopyroxene based on partitioning data from coexisting pyroxenes from the Bishop Tuff (*Hildreth*, 1979).

§ K_d values for Ga and Be are estimated

ferred K_d values used in this study are based mainly on those determined by *Mahood* and *Stimac* (1990), and are listed in Table 5. For Be and Ga, however, suitable K_d data are not available, and estimates are given in Table 5 assuming moderate compatibility with calcic feldspar (i.e. K_d's between Eu and Rb).

The results of FC and AFC modelling using the calculated phase proportions (Table 4) are shown as trace element plots (Fig. 5), and some representative trace element data are listed in Table 4. With some exceptions, most trace elements are satisfactorily modelled by the AFC process provided small amounts of accessory phases participate as fractionating phases. For the trachyandesite → trachyte stage (Fig. 5a) a good fit is obtained for the AFC-2 model, however, for a purely crustal assimilant (AFC-1 model) a poor fit is obtained. This result implies that the trachyandesite compositions used in the modelling (an average of several late-stage trachyandesites) may not be an entirely suitable analog for the less differentiated magma from which the trachytes were derived, at least as far as some trace elements are concerned. Nevertheless, the modelling suggests that a suitable parental composition could be generated by mixing between the trachyandesite liquid and a small

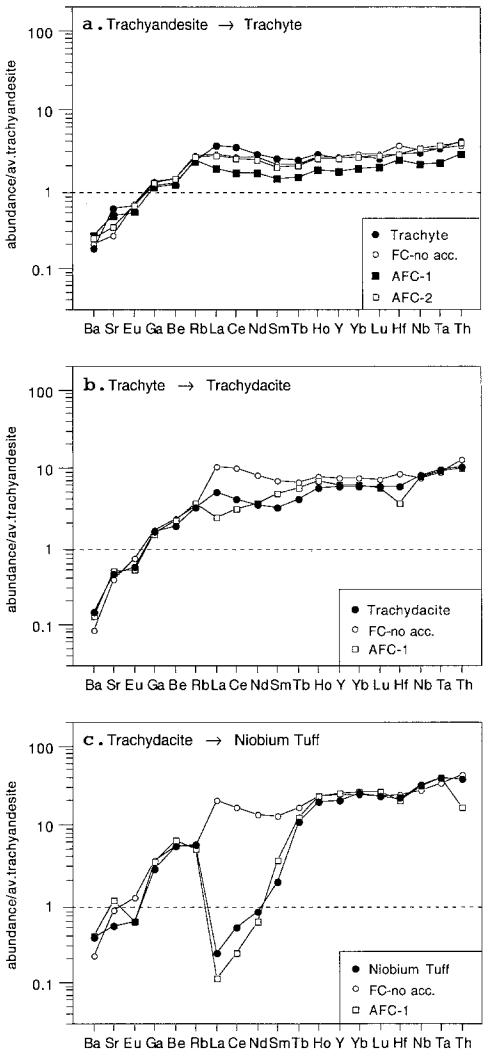

Fig. 5. Plots of observed and modelled trace element distributions for the three evolutionary stages: **a** trachyandesite → trachyte; **b** trachyte → trachydacite, and **c** trachydacite → Niobium Tuff. Element order is based on compatibility with calcic feldspar. *FC-no acc.* fractionational crystallization model with no accessory phase fractionation. *AFC-1* assimilation-fractional crystallization model for assimilant-1. *AFC-2* assimilation-fractional crystallization model for assimilant-2. Both AFC models include accessory zircon and allanite (see Table 4)

proportion of an earlier, more evolved liquid. Such contamination is not unreasonable in a magma chamber which has experienced more than one magma input/differentiation cycle.

For the trachyte → trachydacite stage (Fig. 5b) the feldspar compatible elements (e.g. Rb, Sr, Eu) provide a good fit for both the FC and AFC models. The lower LREE, Hf, and Th abundances in the trachydacite, compared with the FC calculations, require involvement of LREE- and HFSE-selective accessory minerals as fractionating phases. In the AFC model which incorporates allanite and zircon as the LREE- and HFSE-selective phases, respectively, an improved, though not exact, fit is obtained for the trace elements and for ZrO_2 (Table 4). The REE distribution in the trachydacite (Fig. 5b), however, suggests that an accessory mineral with more Ce-to-Sm selectivity compared with allanite is required to achieve a better match between calculated and observed trace element distributions.

For the trachydacite → Niobium Tuff stage FC model (Fig. 5c) more extreme divergence exists between calculated and observed LREE abundances in the absence of any accessory phase fractionation. Although the observed LREE-depletion in the Niobium Tuff can be satisfactorially modelled by fractionation of $\approx 0.25\%$ allanite, a large discrepancy exists between calculated and observed Th abundance (see Table 4).

5 Discussion

5.1 Element modelling by crystal-liquid processes

Fractional crystallization and AFC modelling of the geochemical evolution of the Brockman magmas shows that rare-metal enrichment in the most extreme differentiates can be accounted for by fractionation of phases such as quartz and sanidine that have low crystal-liquid K_d's for the HFSE and HREE. The dominant fractionating phases determined in the models (i.e. calcic feldspar followed by alkali feldspar and quartz) are also consistent with the phenocryst and microphenocryst phases preserved in the rocks (*Taylor* et al., 1995). Calculated calcic feldspar compositions (Table 4) are equivalent to relatively *Or*-rich (26–32 mol%) anorthoclases rather than plagioclase, while the alkali feldspar compositions are equivalent to sodic sanidines. Despite some uncertainty in bulk compositions introduced by secondary modification of Na_2O/K_2O ratios in the Brockman lavas, these calculated feldspar compositions are not atypical of those found in trachyte magmas (cf. *Mahood* and *Stimac*, 1990).

For the mafic phases, the modelled pyroxene compositions show increasing En component with increasing degrees of fractionation, while the titanomagnetites show increasing proportion of magnetite component. Although Fe_2O_3 and FeO were not explicitly modelled in the FC and AFC calculations, these variations are both consistent with increasing magmatic oxidation state during fractionation.

5.2 Accessory phase fractionation versus secondary processes in REE modelling

An important aspect of crystal-liquid fractionation models is the requirement for the fractionation of small amounts (<0.5 wt%) of accessory phases to explain

anomalies in trace element distributions, particularly for the LREE. It may be argued that these phases are not present as phenocrysts so cannot be fractionated, however, it has been shown that accessory minerals may crystallize as inclusions in other fractionating phases, such as feldspar, due to non-equilibrium concentration gradients occurring at the mineral-melt interface during phenocryst growth (*Watson* and *Green*, 1982). In the Brockman magmas, apatite, zircon, and other LREE-selective minerals may have been fractionated in this way.

The exact nature of the LREE-selective mineral or minerals required by the crystal-liquid models is, however, uncertain. The models presented here with allanite as the LREE-selective phase yield trace element distributions that provide a close, but not an exact match. For the trachyte → trachydacite stage it is possible that better agreement between calculated and observed REE distributions may be obtained if another LREE-selective phase was also fractionated. One candidate is monazite which occurs as an accessory phase in the Brockman lavas, and potentially has more middle REE selectivity than allanite (*Mariano*, 1989); the few monazite-liquid K_d determinations in the literature (e.g. *Congdon* and *Nash*, 1991), however, are not of sufficient quality to permit quantitative modelling.

For the trachydacite → Niobium Tuff stage in which the LREE are strongly depleted, allanite fractionation can account for LREE abundances but Th abundance is poorly modelled due to the high Th selectivity of allanite. Monazite is even more Th-selective than allanite (*Congdon* and *Nash*, 1991), and therefore is also unlikely to be a fractionating phase in this case. Although there are a few LREE-minerals occurring in the Brockman volcanics that are not Th-selective, i.e. bastnaesite and related fluorocarbonates, it is difficult to envisage a fluorocarbonate mineral as a primary magmatic precipitate in silicic volcanic rocks of this kind.

The operation of secondary processes in the post-magmatic or regional metamorphic regime offers the best alternative explanation for the marked LREE depletion in the Niobium Tuff. It has recently been shown that the REE can be quite mobile under some conditions of low-T hydrothermal alteration of volcanic rocks (*Kuschel* and *Smith*, 1992), but the mobility does not show strong HREE/LREE selectivity suggesting mineralogical controls are important in the case of the Niobium Tuff. A likely hypothesis, discussed by *Ramsden* et al. (1993), is that the LREE were lost from the Niobium Tuff by selective fluid leaching of secondary fluorocarbonate minerals which are the major LREE host in the Niobium Tuff. The HREE and Th have been unaffected by this process since they occur dominantly in solid-solution in the mineraloid gel-zircon, a phase that does not appear to have been susceptible to fluid leaching under the same conditions. This view is supported by lower La/Sm ratios in fluorocarbonates from the Niobium Tuff compared with those from the trachydacite lavas (*Ramsden* et al., 1993). As with the crystal-liquid model, this explanation is also consistent with the undisturbed REE pattern of the underlying sediment (Fig. 3) in which fluorocarbonate minerals are absent. Because the crystal-liquid model is unable to account for both Th and LREE abundances, and the REE are unlikely to be fractionated by fluid-melt processes (see below), this model must be regarded as the favoured explanation for the extreme LREE-depletion in the Niobium Tuff. However, this explanation is unlikely to apply to the trachydacites which have a different pattern of LREE "depletion" (Fig. 5b) and contain monazite as the dominant LREE mineral. A crystal-liquid model involving accessory phase fractionation is favoured in this case.

5.3 *Liquid fractionation*

An important observation from the major and trace element modelling is that very large degrees of crystallization are apparently required to generate the most evolved Brockman liquids. In fact, to derive the Niobium Tuff composition, $\approx 98\%$ crystallization of the starting trachyandesite liquid is required. Since the trachyandesite itself would have been derived from a more primitive mafic composition, the Niobium Tuff represents an extreme differentiate ($< 1\%$) of a hypothetical primitive liquid parental to the Brockman volcanics. The question arises as to whether such a large degree of crystallization is physically reasonable.

Derivation of the Brockman volcanics by simple crystal settling processes requires crystallization of unrealistically large volumes of a parental magma body. At Brockman, and other trachytic volcanic localities, there is little evidence for the existence of extensive volumes of magmatic cumulates at depth. To overcome such problems, *Sparks* et al. (1984) and *McBirney* et al. (1985) proposed that highly evolved liquids can be derived by a process termed "liquid fractionation" (or "convective fractionation") involving modest degrees of crystallization of a convecting magma body. In this mechanism, liquids evolve by crystallization at a boundary layer on the walls of the magma chamber where they form less dense, buoyant, derivative liquids that rise along the boundary layer. Vertical gradients in composition and physical properties exist in liquids near the boundary layer due to magma mixing and/or diffusional controls. During roofward flow, the buoyant liquids continue to fractionate and, depending on their density constrast, they may segregate into separate gravitationally stable layers so leading to internal compositional stratification of the magma chamber. The major advantages of the liquid fractionation model are that no extraordinary processes are required to account for very high degrees of differentiation and a mechanism exists for rapid development of chemical zonation within the upper portion of the magma chamber. Also the differentiation of the magmas, essentially at the country-rock/magma body interface, allows ready incorporation of wall-rock-derived contaminants.

The high degrees of differentiation, the presence of several essentially discrete magma compositions, and the requirement for country-rock contamination are all evidence pointing to the operation of liquid fractionation processes in the evolution of the Brockman magmas. In alkaline systems, magma segregation is believed to begin only when parental magmas have crystallized sufficiently to form residual liquids of broadly trachyte composition (i.e. ≈ 60 wt% silica; *Baker* and *McBirney*, 1985). In the Brockman magma chamber, it can be envisaged that trachyte and trachydacite liquids may have segregated into separate compositional layers above the main body of the magma chamber composed of trachyandesitic liquids. Such stratification in the magma chamber could account for the discrete magma compositions seen in geochemical evolution diagrams (Figs. 1, 4). Alternatively, the trachytes and trachydacites may have formed in separate liquid fractionation episodes in which the magma chamber was replenished by fresh parental liquids after eruption of the previous upper zone. Magma mixing between differently evolved liquids in the Brockman magma chamber may also have taken place as suggested by the AFC modelling.

During cooling of the magma body the compositional interfaces generated by liquid fractionation will gradually be eliminated. However, as pointed out by *Baker*

and *McBirney* (1985), static crystallization of magma under the roof of the chamber may evolve small volumes of low-density, volatile-enriched liquids having extreme compositions. It is probable that liquids of Niobium Tuff composition were generated in such a roof-zone environment.

5.4 The role of fluorine in melt-related processes

Because of probable devitrification losses and secondary mobilization, the original F content of the Brockman lavas and Niobium Tuff cannot be determined precisely (cf. *Webster*, 1990). Nevertheless, F contents for the most evolved Brockman volcanics of ≈ 0.3–0.5 wt% for the trachydacites and ≈ 1.5–2 wt% for the Niobium Tuff, indicate that the Brockman magmas evolved under conditions of relatively high-magmatic f_{F2}. Such conditions are likely to have contributed significantly to incompatible element enrichments. In silicic melts, fluorine has an important effect in lowering crystal-liquid K_d's (*Green* et al., 1992) and in expanding the above-solidus phase volumes of quartz and sanidine (*Bailey*, 1977) both of which phases have low crystal-melt K_d's for HFSE and REE elements. F(luorine) also increases the crystallization interval (i.e. solidus to liquidus range) of rhyolitic compositions and reduces the solidus temperature to ≈ 500–600°C depending on water content (*Bailey*, 1977; *Webster* et al., 1987). This increases the temperature range and hence the period over which active crystal fractionation can take place in a cooling magma body. Lastly, high F solubility results in an increase in the diffusivities of melt components, and a decrease in both melt denisties and melt viscosities (*Dingwell* et al., 1985, 1993). This effectively offsets temperature-related diffusivity and viscosity changes caused by decreasing magmatic temperature which would otherwise limit the efficiency of crystal-melt separation.

Diffusion-controlled differentiation assisted by fluoride complexation has been proposed as an additional mechanism by which melts may be enriched in so-called "fluorophile" elements such as Be, Zr, Nb, HREE, U, Sn and Li (e.g. *Mahood*, 1981). The operation of such processes might be suspected for elements having anomalous distributions, i.e. those that cannot be explained by FC or AFC processes. None of the fluorophile elements in the Brockman volcanics, however, show anomalous abundances that could be used as evidence to support such a process. In addition, there is no evidence that other non-crystal-liquid processes, such as silicate-fluoride immiscibility, played a role in the genesis of the Brockman volcanics. This is consistent with the absence of phase separation in topaz rhyolite melts containing up to 6 wt% F (*Webster*, 1990).

5.5 The role of fluorine in fluid-related processes

Fluorine-bearing hydrothermal fluids can be important agents in the transport of rare-metals during near-solidus crystallization of granitic systems (e.g. *Gunow* et al., 1980; *London*, 1990), or during subsolidus devitrification of glassy rhyolites (e.g. *Webster* and *Holloway*, 1990). However, element partitioning studies on fluid-saturated, F-rich rhyolite compositions under above-solidus conditions by *London* et al. (1988), indicate that none of the fluorophile elements show preferential partitioning into the fluid phase (i.e. they have fluid-melt K_d's < 1), and the HREE are not strongly fractionated relative to the LREE.

In the post-magmatic regime, e.g. during devitrification of an F-rich rhyolitic tuff, *Bailey* (1977) has suggested that fluorophile rare-metals may be transported as fluoride and hydroxy-fluoride complexes in a fluid phase, although this view is controversial (see *London*, 1987). In the case of the Niobium Tuff, with the exception of F, there is little evidence for any significant fluid transport of ore-forming components into the immediate country rocks. "Except for late fluid leaching of LREE from fluorocarbonates," ore-forming elements in the Niobium Tuff appear to have been mobilized and re-precipitated as secondary minerals essentially within the confines of the Niobium Tuff horizon (see *Ramsden* et al., 1993).

5.6 Parent magma composition and mantle source affinity

The positive ε_{Nd} signature of the Brockman volcanics indicate they were not derived from partial melting of older granitic crust in contrast to other rare-metal-enriched volcanics such as the topaz rhyolites of North America (*Christiansen* et al., 1986). Instead, the ε_{Nd} signature of the trachyandesites, which show the least effects of crustal contamination, indicate that the Brockman parent magma had an initial ε_{Nd} value $> +2.6$. In terms of isotopically distinct mantle sources, this is consistent with an origin from "PREMA"-type mantle material (*Zindler* and *Hart*, 1986), which is characterized by ε_{Nd}(present-day) $\approx \pm 5$. In Tertiary to recent volcanic environments, intraplate oceanic and continental "hot-spot" volcanic provinces such as Hawaii, Iceland and Eastern Australia are of PREMA derivation (*Zindler* and *Hart*, 1986; *Sun* et al., 1989), suggesting that Proterozoic magmatism at Brockman was also of this intraplate type. This view is supported source-diagnostic incompatible trace element ratios such as Zr/Nb and Nb/La (see *Sun* and *McDonough*, 1989). For the trachyandesites, Zr/Nb $\approx$ 6–8 and Nb/La $\approx$ 1.1–1.3, which indicate the Brockman volcanics have closest affinity with Ocean Island Basalt (OIB) "hot-spot"-type mantle sources (av. Zr/Nb $\approx$ 6, Nb/La $\approx$1.3) rather than with a MORB source (av. Zr/Nb $\approx$ 32, Nb/La $\approx$ 0.9).

In terms of whole-rock geochemistry, it is likely that the Brockman parent magma was basaltic with relatively high K_2O/Na_2O and *Hy/Di* ratios, and transitional silica saturation levels (i.e. *Ol-Hy-Di* normative). Compositions very similar to the Brockman trachyandesites can in fact be modelled as derivatives of some OIB basalts, such as those from Gough Island (*Weaver* et al., 1987), by fractionation of largely olivine and clinopyroxene. However, Gough Is. basalts are derived from an enriched mantle or EM source, and are therefore isotopically distinct from the postulated Brockman parent. The nature of the Brockman parent magma is therefore somewhat enigmatic compared with modern intraplate basaltic magmas. This view is reinforced by the fact that no modern basaltic provinces of PREMA derivation have produced Qz-normative differentiated magmas with the extreme levels of incompatible element enrichment found at Brockman.

Acknowledgements

The authors would like to thank *I. Chalmers* and *T. Ramsted* (Multimetal Consultants Pty Ltd, Perth) for their helpful comments and logistical support in the field. Dr. *R. Chang* and *C. Twist* (University of Western Australia) are thanked for their assistance in the analytical laboratory, and Drs. *N. Rock* (deceased), *E. Mikucki* (University of Western Australia) and

J. Stolz (University of Tasmania) kindly commented on earlier drafts of this manuscript and Dr. *B. Collins* provided thoughtful referee comments. S.-S. Sun publishes with the permission of the Director, Australian Geological Survey Organisation, Canberra. This study was supported by a University of Western Australia special research grant to *N. M. S. Rock* and *W. R. Taylor*, and by Australian Research Council funding to *W. R. Taylor* (University of Tasmania).

References

Bailey JC (1977) Fluorine in granitic rocks and melts: a review. Chem Geol 19: 1–42

Baker BH (1987) Outline of the petrology of the Kenya rift alkaline province. Geol Soc Lond Special Publ 30: 239–311

Baker BH, McBirney AR (1985) Liquid fractionation, part III. Geochemistry of zoned magmas and the compositional effects of liquid fractionation. J Volcanol Geotherm Res 24: 55–81

Brooks CK, Henderson P, Rønsbo JG (1981) Rare-earth partition between allanite and glass in the obsidian of Sandy Braes, Northern Ireland. Min Mag 44: 157–160

Burt DM, Bikun JV, Christiansen EH (1982) Topaz rhyolites—distribution, origin and significance for exploration. Econ Geol 77: 1818–1836

Cameron KL (1984) The Bishop Tuff revisited: new rare earth element data consistent with crystal fractionation. Science 244: 1338–1340

Christiansen EH, Bikun JV, Sheridan MF, Burt DM (1984) Geochemical evolution of topaz rhyolites from the Thomas Range and Spor Mountain, Utah. Am Min 69: 223–236

Christiansen EH, Sheridan MF, Burt DM (1986) The geology and geochemistry of Cenozoic topaz rhyolites from the western United States. Geol Soc Am Special Paper 205: 79p

Congdon R, Nash WP (1991) Eruptive pegmatite magma: rhyolite of the Honeycomb Hills, Utah. Am Min 76: 1261–1278

Dingwell DB, Scarfe CM, Cronin DJ (1985) The effect of fluorine on viscosities in the system Na_2O–Al_2O_3–SiO_2: implications for phonolites, trachytes and rhyolites. Am Min 70: 80–87

Dingwell DB, Knocke R, Webb SL (1993) The effect of F on the density of haplogranite melt. Am Min 78: 325–330

Esslemont G (1990) The geology and geochemistry of the Brockman alkaline volcanics and rare-metal deposit. Thesis, University of Western Australia (unpublished)

Ewart A, Chappell BW, LeMaitre RW (1985) Aspects of the mineralogy and chemistry of the intermediate-silicic Cainozoic volcanic rocks of eastern Australia, part 1. Introduction and geochemistry. Aust J Earth Sci 32: 359–382

Ewart A, Chappell BW (1989) Trace element geochemistry. In: *Johnson RW* (ed) Intraplate volcanism in Eastern Australia and New Zealand. Cambridge University Press, Cambridge, pp 219–235

Francalanci L (1989) Trace element partition coefficients for minerals in shoshonitic and calc-alklaine rocks from Stromboli Islands (Aeolian Arc). Neues Jahrb Miner Abh 160: 229–247

Gunow AJ, Ludington S, Munoz JL (1980) Fluorine in micas from the Henderson molybdenite deposit, Colorado. Econ Geol 75: 1127–1137

Green TH, Adam J, Sie S (1992) Trace element partitioning and mantle metasomatism. Geol Soc Aust Abstracts 32: 186–187

Hildreth W (1979) The Bishop Tuff: evidence for the origin of compositional zonation in silicic magma chambers. In: *Chapin CE, Elston WE* (eds) Ash-flow tuffs. Geol Soc Am Special Paper 180, pp 43–75

Kampunzu AB, Mohr P (1991) Magmatic evolution and petrogenesis in the East Africa Rift system. In: *Kampunzu AB, Lubala RT* (eds) Magmatism in extensional structural settings—the Phanerozoic African plate. Springer, Berlin Heidelberg New York Tokyo, pp 85–136

Kuschel E, Smith IEM (1992) Rare earth mobility in young arc-type volcanic rocks from northern New Zealand. Geochim Cosmochim Acta 56: 3951–3955

LeMaitre RW (1989) A classification of igneous rocks and glossary of terms. Blackwells Scientific Publications, Oxford, 193p

London D (1987) Internal differentiation of rare-element pegmatities: effects of boron, phosphorus, and fluorine. Geochim Cosmochim Acta 51: 403–420

London D, Hervig RL, Morgan GB (1988) Melt-vapour solubilities and element partitioning in peraluminous, granite-pegmatite systems; experimental results with Macusani glass at 200 MPa. Contrib Mineral Petrol 99: 360–373

London D (1990) Internal differentiation of rare-element pegmatites; a synthesis of recent research. In: *Stein HJ, Hannah JL* (eds) Ore-bearing granite systems; petrogenesis and mineralizing processes. Geol Soc Am Special Paper 246, pp 35–50

Maas R, McCulloch MT (1991) The provenance of Archean clastic metasediments in the Narryer Gneiss Complex, Western Australia: trace element geochemistry, Nd isotopes and U–Pb ages for detrital zircons. Geochim Cosmochim Acta 55: 1915–1932

Macdonald R (1987) Quaternary peralkaline silicic rocks and caldera volcanoes of Kenya. In: *Fitton JG, Upton B* (eds) Alkaline igneous rocks. Geological Society Special Publication 30, pp 313–333

Mahood GA (1981) Chemical evolution of a Pleistocene rhyolitic center. Sierra La Primavera, Jalisco, Mexico. Contrib Mineral Petrol 52: 175–191

Mahood GA, Stimac JA (1990) Trace-element partitioning in pantellerites and trachytes. Geochim Cosmochim Acta 54: 2257–2276

Mariano AN (1989) Economic geology of rare-earth minerals, In: *Lipin BR, McKay GA* (eds) Geochemistry and mineralogy of rare-earth elements. Rev Mineral 21, pp 309–337

McBirney AR, Baker BH, Nilson RH (1985) Liquid fractionation, part I. Basic principles and experimental simulations. J Volcanol Geotherm Res 24: 1–24

Miyashiro A (1978) Nature of alkalic volcanic rock series. Contrib Mineral Petrol 66: 91–104

Nabelek PI, Russ-Nabelek C (1990) The role of fluorine in the petrogenesis of magmatic segregations in the St. Francois volcano-plutonic terrane, southeastern Missouri. In: *Stein HJ, Hannah JL* (eds) Ore-bearing granite systems; petrogenesis and mineralizing processes. Geol Soc Am Special Paper 246, pp 71–87

Pearce JA, Norry MJ (1979) Petrogenetic implications of Ti, Zr, Y and Nb variations in volcanic rocks. Contrib Mineral Petrol 69: 33–47

Ramsden AR, French DH, Chalmers DI (1993) The volcanic-hosted rare-metals deposit at Brockman, Western Australia: mineralogy and geochemisty of the Niobium Tuff. Mineral Deposita 28: 1–12

Sawka WN, Chappell BW (1988) Fractionation of uranium, thorium and rare earth elements in a vertically zoned granodiorite: implications for heat production distributions in the Sierra Nevada batholith, California, U.S.A. Geochim Cosmochim Acta 52: 1131–1143

Scott RB (1971) Chemical variations in glass shards and interstitial dust of ignimbrite cooling units. Am J Sci 270: 166–173

Sparks RS, Huppert HE, Turner JS (1984) The fluid dynamics of evolving magma chambers. Phil Trans Roy Soc Lond A310: 511–534

Stolz AJ (1985) The role of fractional crystallization in the evolution of the Nandewar Volcano, north-eastern New South Wales, Australia. J Petrol 26: 1002–1026

Sun S-S, McDonough WM (1989) Chemical and isotopic systematics of ocean basalts: implications for mantle compositions and processes. Geol Soc Lond Special Publ 42: 313–345

Sun S-S, McDonough WM, Ewart A (1989) A four-component model for East Australian basalts. In: *Johnson RW* (ed) Intraplate volcanism in Eastern Australia and New Zealand. Cambridge University Press, Cambridge, pp 333–347

Taylor SR, McClennan SM (1985) The continental crust: its composition and evolution. Blackwell Scientific Publications, Oxford, 312p

Taylor WR, Page RW, Esslemont G, Rock NMS, Chalmers DI (1995) Geology of the Brockman rare-metals deposit, Halls Creek Mobile Zone, northwest Australia. I. Volcanic environment, geochronology and petrography of the Brockman volcanics. Mineral Petrol 52: 209–230

Weaver BL, Wood DA, Tarney J, Joron JL (1987) Geochemistry of ocean island basalts from the South Atlantic: Ascension, Bouvet, St. Helena, Gough and Tristan da Cunha. Geol Soc Lond Special Publ 30: 253–267

Webster JD (1990) Partitioning of F between H_2O and CO_2 fluids and topaz rhyolite melt. Contrib Mineral Petrol 104: 424–438

Webster JD, Holloway JR, Hervig RL (1987) Phase equilibria of a Be, U, and F-enriched vitrophyre from Spor Mountain, Utah. Geochim Cosmochim Acta 51: 389–402

Webster JD, Holloway JR (1990) Partitioning of F and Cl between magmatic hydrothermal fluids and highly evoloved granitic magmas. In: *Stein HJ, Hannah JL* (eds) Ore-bearing granite systems; petrogenesis and mineralizing processes. Geol Soc Am Special Paper 246, pp 21–34

Webster JD, Duffield WA (1991) Volatiles and lithophile elements in Taylor Creek Rhyolite: constraints from glass inclusion analysis. Am Min 76: 1628–1645

Wörner G, Schmincke H-U (1984) Mineralogical and chemical zonation of the Laacher See tephra sequence (East Eifel, W. Germany). J Petrol 25: 805–835

Zindler A, Hart S (1986) Chemical geodynamics. Ann Rev Earth Planet Sci 14: 493–571

Yates KR, Pontifex IR (1973) Geological investigation of niobium-bearing rocks in temporary reserve 5715H, Halls Creek, Western Australia. Report, Trend Exploration Pty Ltd, 24p (unpublished)

Authors' address: Dr. *W. R. Taylor*, Department of Geological Sciences, University College London, Gower Street, London WC1E 6BT, United Kingdom